Simulating the energy savings potential in domestic heating scenarios in Switzerland

Wilhelm Kleiminger[1], Silvia Santini[2], and Friedemann Mattern[1]

[1] Institute for Pervasive Computing, ETH Zurich, 8092 Zurich, Switzerland
{wilhelmk,mattern}@inf.ethz.ch
[2] Wireless Sensor Networks Group, TU Darmstadt, 64283 Darmstadt, Germany
silvia.santini@wsn.tu-darmstadt.de

Abstract. This report presents a simulation framework based on the ISO 13790 5R1C lumped capacitance building model for the evaluation of the energy savings potential of occupancy prediction algorithms. We show the derivation of the model parameters and introduce a new methodology to prepare weather data for simulating the energy consumption of a heating system when predictively controlling the thermostat.

1 Introduction

Heating accounts for a large share of the energy expenditure in moderate climates such as Switzerland [15]. When the outside temperature drops below the desired indoor temperature, heating is necessary since buildings lose thermal energy to the surroundings through radiation, transmission and ventilation. Especially, as the difference between the indoor and outside temperature becomes larger, the amount of energy lost to the environment increases [11].

Smart heating systems aim at saving energy by automatically lowering the temperature while the home is unoccupied. However, these systems need a prediction of the return time of the occupants' to decide when to start pre-heating a building in order for it to reach a comfortable temperature upon their arrival. The accuracy of this prediction directly affects the amount of energy that may be saved and the amount of comfort lost due to mis-predictions of the arrival time of the occupants. Previous research has evaluated occupancy prediction algorithms in a variety of different settings. Several authors show the results of simulations [5,17,18], while others report findings from real world deployments [8,21]. While there certainly is no lack of models to simulate the energy consumption of a building, few authors have compared their work to other existing algorithms using the same model and dataset.

In this report we present a framework for the simulation of the energy savings achieved by a smart heating system with a predictive controller that heats a building based on a predicted occupancy schedule. In Section 2 we introduce the lumped capacitance model to calculate transient heat transfer and go on to describe the 5-resistance 1-capacitance (5R1C) model of the ISO 13790 standard [13]. In Section 3 we show how using real meteorological data from 20 years, we developed characteristic weather scenarios that may be used to evaluate the impact of various occupancy prediction algorithms. In Section 4, we focus on the parametrisation of the 5R1C model for four fictitious buildings in Lausanne, Switzerland. We show the calculation of the heat losses due to transmission and ventilation, as well as the heat gains due to internal gains, solar gains and the heating system. In Section 5 we introduce the predictive controller used to translate predicted occupancy schedules into commands for the thermostat and discuss some limitations of the 5R1C model in Section 6. The simulation framework described in this report has been used to analyse and compare various occupancy prediction strategies for smart heating systems [16].

2 Lumped capacitance models

In building design, the indoor temperature may be modelled as a transient heat transfer problem. A simple example for transient conduction (i.e. heat transfer that is time dependent) is a banana

cake taken out of the oven and left to cool down in the kitchen. Energy is transferred from the surface of the cake to its surroundings by convection and radiation. At the same time conduction also occurs between the interior of the cake and its surface. The energy transfer occurs as long as the cake has not reached a steady state temperature distribution.

One of the simplest models for describing such transient conduction is the *lumped capacitance model* [11]. The lumped capacitance model makes the simplifying assumption that there is no temperature gradient within the solid. Thus, the temperature on the surface of the cake is assumed to be the same as the interior temperature. This is clearly impossible as it would imply the existence of infinite thermal conductivity in the cake. However, this is well approximated if the internal conductivity in the cake is higher than the conductivity to the surroundings.

When looking at a building scenario, the rate of heat loss $\dot{E_{out}}$ of the building must be the same as the rate of change of its internal energy $\dot{E_{st}}$. This may be written as:

$$-\dot{E_{out}} = \dot{E_{st}} \tag{1}$$

However, when considering the indoor temperature, we are not merely interested in reaching the steady state temperature distribution of the building with the outside as it cools down. Instead we want to know how much energy must be spent to keep the building at a comfortable temperature level and how long it takes to heat up to this level. Thus we must counteract the rate of change of the internal energy $\dot{E_{st}}$ by introducing heat gain $\dot{E_{in}}$ into the system. Figure 1 shows the simple resistance-capacitance circuit used for this purpose.

$$\dot{E_{in}} = \dot{E_{out}} + \dot{E_{st}} \tag{2}$$

Introducing the temperature difference between the indoor Θ_{in} and outside temperatures Θ_e, the equation may be re-written as:

$$\dot{E_{in}} = \frac{\Theta_{in} - \Theta_e}{R} + C\frac{d\Theta_{in}}{dt} \tag{3}$$

where R stands for the thermal resistance ($R = \frac{1}{hA_s}$) and C for the thermal capacitance ($C = \rho V c$) of the building components facing the outside, respectively. Table 1 shows the definition of all parameters.

Table 1. Variables used in calculation of transient heat transfer with the lumped capacitance model.

Variable	Description
$\dot{E_{out}}$	Heat loss (W)
$\dot{E_{in}}$	Heat gain (W)
$\dot{E_{st}}$	Heat stored (W)
Θ_{in}	Indoor temperature (K)
Θ_{out}	Outside temperature (K)
R	Thermal resistance (K/W)
C	Thermal capacitance (J/K)
h	Heat transfer coefficient ($W/(m^2K)$)
A_s	Surface area (m^2)
ρ	Density (kg/m^3)
V	Volume (m^3)
c	Specific heat ($J/(kgK)$

Now equation (3) may be rewritten as:

$$\frac{d\Theta_{in}}{dt} + \frac{\Theta_{in}}{RC} = \frac{\dot{E_{in}}R + \Theta_e}{RC} \tag{4}$$

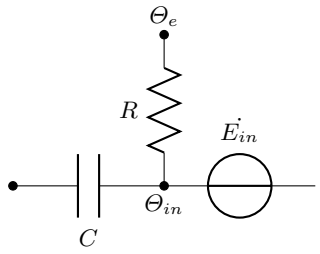

Fig. 1. Simple 1R1C model.

Multiplying by integrating factor $e^{\int \frac{1}{RC} dt} = e^{\frac{t}{RC}}$ and applying the product rule in reverse gives:

$$\int \frac{d\Theta_{in}}{dt} e^{\frac{t}{RC}} = \int \frac{\dot{E_{in}} R + \Theta_e}{RC} e^{\frac{t}{RC}} \tag{5}$$

$$\Theta_{in}(t) = (\dot{E_{in}} R + \Theta_e) + D e^{\frac{-t}{RC}} \frac{\dot{E_{in}} R + \Theta_e}{RC} \tag{6}$$

Fixing $\Theta_{in}(0) = \Theta_{in}(t-1)$ for $t = 0$ we can calculate D:

$$\Theta_{in}(t-1) = (\dot{E_{in}} R + \Theta_e) + D \frac{\dot{E_{in}} R + \Theta_e}{RC} \tag{7}$$

Substituting D in $\Theta_{in}(t)$ gives the indoor temperature at time t – $\Theta_{in}(t)$ – as a function of the indoor temperature at the previous interval $\Theta_{in}(t-1)$, the outside temperature Θ_e, the resistance and capacitance values (R and C) and the heat added to the system $\dot{E_{in}}$:

$$\Theta_{in}(t) = \Theta_{in}(t-1) e^{\frac{-t}{RC}} + (\dot{E_{in}} R + \Theta_e)(1 - e^{\frac{-t}{RC}}) \tag{8}$$

2.1 ISO 13790 5R1C model

One of the first to advocate the use of electric circuits to simulate the energy consumption of a heating system was Clemens Beuken, who introduced the concept in his 1936 PhD thesis on the "Heat loss in periodically powered ovens" [2]. In the Beuken method, the electric voltage corresponds to the temperature and the electric current is equivalent to the heating flux q.

Today this method has been standardised in the EN ISO 13790 energy performance standard and adopted extensively for building simulations in Europe [3,14]. The standard was mandated by the EU Directive 2002/91/EC on the energy performance of buildings (EPBD) which required a "*common methodology for calculating the integrated energy performance of buildings*" [6]. To simulate the hourly energy expenditure, the ISO 13790 standard includes a 5 resistance, 1 capacitance model (5R1C). This RC circuit for the 5R1C model is shown in Figure 2. The most significant parameters used by the model are listed in Table 2. The RC circuit models the transient conduction between the property and its surroundings and offers a method to calculate the energy needs for heating and cooling while maintaining specified set-point temperatures. In contrast to the simple 1R1C model derived in the previous section and used for example in [18], the 5R1C model takes into account the heat transfer by transmission and ventilation as well as solar and internal gains. The model also allows for the calculation of the mean transient air temperature Θ_{air}, the mean radiant (masonry) temperature Θ_m and the internal surface temperature Θ_s.

3 Weather scenarios

In this report we use actual weather data for calibrating the 5R1C model for the design heat load and for simulating different environmental conditions. To set up the system, we use 20 years of weather

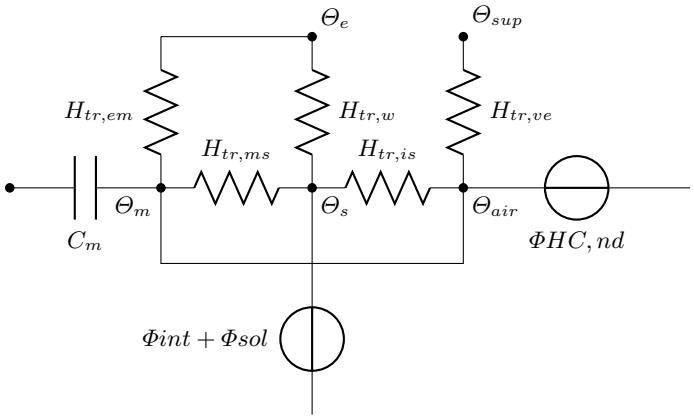

Fig. 2. ISO 13790 5R1C model.

Table 2. Excerpt of ISO 13790 5R1C parameters.

Symbol	Units	Description	Notes
		Output	
Θ_m	°C	Mean radiant (masonry) temperature	
Θ_{air}	°C	Mean air temperature	
		Input	
$\Theta_{int,H,set}$	°C	Heating setpoint temperature	$\Theta_{comfort} = 20\,°C$, $\Theta_{setback} = 10\,°C$
$\Theta_{int,C,set}$	°C	Cooling setpoint temperature	
$\Theta_{m,0}$	°C	Mean radiant temperature at time $t = 0$	
Θ_e	°C	Outside temperature	
Θ_{sup}	°C	Temperature of ventilation air	$\Theta_{sup} = \Theta_e$
$\Phi_{HC,nd}$	W	Actual heat input	$\Phi_{HC,nd}$ in ISO 13790 covers heating and cooling
$\Phi_{H,max}$	W	Maximum heating input	
Φ_{int}	W	Internal heat gains	
Φ_{sol}	W	Solar heat gains	
H_{ve}	K/W	Ventilation heat transmission coefficient	
$H_{tr,w}$	K/W	Transmission heat transfer coefficient (windows, doors)	
$H_{tr,op}$	K/W	Transmission heat transfer coefficient (opaque elements)	
C_m	J/K	Thermal capacitance of building mass	
A_f	m^2	Floor area	

data from Pully, Switzerland (close to Lausanne) to find Θ_d, the norm outside temperature, and $\Theta_{m,e}$, the yearly mean of the outside temperature. Both are used in Section 4.2 for the calculation of the design heat load Φ_H. The weather data has been provided by the Swiss Federal Office of Meteorology and Climatology (MeteoSwiss).[3] For details of the design heat load calculation the reader is referred to Section 4.2. Table 4 shows the weather data used in this report. We use this data to design different environmental scenarios based on the distribution of the outside temperature.

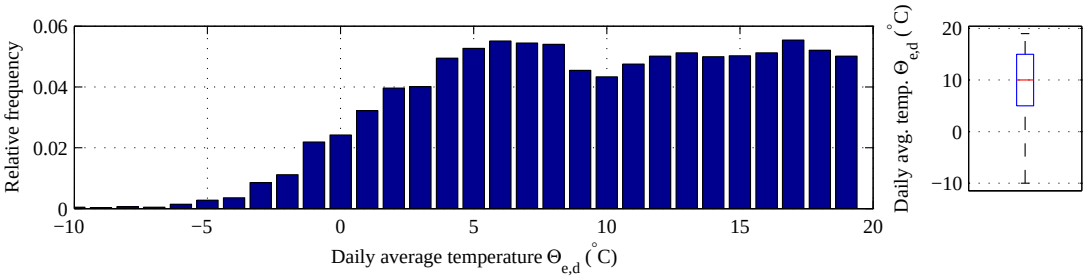

Fig. 3. Distribution of daily average temperature $\Theta_{e,d}$ in Pully, Switzerland (Jan 1994 to Jan 2014). $\Theta_{e,d} \geq 20\,°\text{C}$ are excluded. Right subfigure shows median and quartiles.

Figure 3 shows the distribution of the daily average temperatures over 20 years from January 1994 to January 2014. To generate possible heating scenarios, we only consider days with an average outside temperature $\Theta_{e,d} < 20$, as only these may contribute to the total heating degree days. The left part of the figure shows that there is a peak in the relative frequency around 6 °C. The small subfigure on the right shows that the median temperature in the observed sample is 10 °C (i.e. 50% of the days requiring heating have temperatures below 10 °C), while the lower quartile is 5 °C (i.e. 25% of the days requiring heating have temperatures below 5 °C). The minimum value observed is −10 °C. Since we have established that the norm outside temperature of our heating system is −6 °C, we do not consider the minimum temperature. This led us to the following 8 test scenarios for our heating simulation:

Table 3. Weather scenarios. For each of the 8 scenarios, the table shows the daily average temperature $\Theta_{e,d}$ and the daily average of the global radiation I_{avg} for reference.

		$\Theta_{e,d}$ (°C)		I_{avg} (W/m^2)	
Scenario	**Range**	**clear**	**cloudy**	**clear**	**cloudy**
Very low temperature	$-6\,°\text{C} \leq \Theta_e \leq -4\,°\text{C}$	-5.4	-4.7	142.9	35.5
Freezing temperature	$-1\,°\text{C} \leq \Theta_e \leq 1\,°\text{C}$	0.1	0.0	137.5	30.2
Low temperature	$4\,°\text{C} \leq \Theta_e \leq 6\,°\text{C}$	5.1	5.1	148.5	26.1
Moderate temperature	$9\,°\text{C} \leq \Theta_e \leq 11\,°\text{C}$	10.1	10.0	180.7	29.7

By choosing the bounds for the *very low* temperature to be slightly above the norm outside temperature, we seek to avoid a scenario where the power of our modelled heating system is insufficient to heat up the property to a comfortable temperature during parts of the day.

The 8 weather scenarios are built using data from January 1, 2005 to January 1, 2014. All calculations on the solar radiation as described in Section 4.5 were done at a granularity of 10 minutes. The resulting dataset was resampled at 15-minute intervals for the simulation. $\Theta_{e,d}$ denotes the daily average of the outside temperature and I_d denotes the daily average of the global radiation. Days with $I_{avg} \geq 100$ have been considered *clear*. Days with $I_{avg} \leq 50$ have been considered *cloudy*. The scenarios were built by considering all days in the dataset which fit the criteria. Figures showing

[3] MeteoSwiss provides a web interface for researchers at `http://gate.meteoswiss.ch/idaweb`.

the actual values for Θ_e and I_{dir} for all scenarios in conjunction with the response of an optimal controller can be found in the appendix.

Table 4. MeteoSwiss dataset: Pully, Switzerland (46 °30′44″, 06 °40′03″).

Variable	Description	From	To
I	Global radiation (10-minute mean)	01/01/2005	01/01/2014
Θ_e	Outside temperature (2m above surface, 10-minute mean)	01/01/1994	01/01/2014

3.1 Weather data and occupancy

In this report we are assuming there is no correlation between the occupancy schedule of a household and the weather conditions. Due to the fact that the occupancy traces from different households do not necessarily cover the same timespan (or have the same length), we cannot compare the energy savings obtained in different households if we were to use weather data corresponding to the actual occupancy data.

3.2 Annual model

In order to estimate how much energy may be saved by a predictive heating system on an annual basis, we must take into account the relative frequency of the weather scenarios and weigh the scenarios accordingly. As Figure 3 shows, the very low temperature scenario with its proximity to the norm outside temperature is not very likely to occur on a typical day. The moderate temperature scenario on the other hand is much more likely to occur. Using the relative frequencies for temperatures below 20 °C shown in Figure 3, we have calculated the probabilities for the different weather scenarios. For this, we extended the ranges shown in Table 3 to the ones in Table 5. This had no effect on the derivation of the scenarios, but made sure that the performance evaluation of the smart heating system covers the temperatures relevant for heating. Thus, Table 5 shows that a temperature between −2.5 °C and 2.5 °C is half as likely than a temperature between 2.5 °C and 7.5 °C. We have extended the ranges of the very low and moderate temperature scenarios to cover the whole range of temperatures.

While this does not affect the low temperature scenario (temperatures under −6 °C do not occur very often), the probability of the moderate scenario is now overestimated in order to cover the temperatures up to 19 °C. Compared to a scenario with equi-sized bounds (i.e. 7.5 °C to 12.5 °C), the probability of the moderate temperature scenario increases from 24% to 63% - an overestimation of 39%.

In order to understand the implications of this one must look at the behaviour of the heating system as the outside temperature increases. For higher temperatures, the absolute available savings drop to zero as Θ_e approaches Θ_{comf} and the solar gains are sufficient to heat the building. Heating becomes unnecessary. At the same time, the relative (percentage) savings increase as shorter preheat times lead to a more reactive heating system (i.e. the heating system can stay in the off state for longer). However, the relative savings are bounded above by the occupancy of the household. Heating can only be forgone when the building is unoccupied. The participants in our dataset are absent from home on average 26% of the day [16]. This means that the average savings are bounded above by 26% as we cannot do better than switching off the temperature during unoccupied periods.

By using the moderate temperature as a model also for temperatures above 12.5 °C we thus both overestimate the total energy spent and underestimate the percentage savings, leading to an acceptable error overall.

3.3 Global weather scenarios

The potential for energy savings achievable by a predictive heating system varies by region. In fact, some more moderate climates may rarely need any heating at all during the year. Moreover, the

Table 5. New ranges for weather scenarios with probabilities. Where ranges overlap, each scenario is assigned one half of the relative frequency of that particular temperature.

Range	Probability (%)	Used weather scenario
$-10 \leq \Theta_e \leq -2.5$	1	Very low temperature
$-2.5 \leq \Theta_e \leq 2.5$	11	Freezing temperature
$2.5 \leq \Theta_e \leq 7.5$	24	Low temperature
$7.5 \leq \Theta_e \leq 19$	63	Moderate temperature

Table 6. Average, average lowest and absolute lowest outside temperatures (Θ_e) in °C for selected cities for January to March. Estimated norm outside temperature (cf. Section 4.2) for the dimensioning of the heating system.

	Avg. Θ_e			**Avg. lowest Θ_e**			**Abs. lowest Θ_e**			**Est. Θ_d**
City	*Jan*	*Feb*	*Mar*	*Jan*	*Feb*	*Mar*	*Jan*	*Feb*	*Mar*	
Moscow	-8	-7	-2	-11	-11	-5	-36	-33	-27	-20.5
Toronto	-5.8	-5.6	-0.4	-10.1	-10.2	-5.3	-35.2	-25.7	-25.6	-18.7
Beijing	-4	-1	6	-8.4	-5.6	0.4	-17	-15	-8	-8.9
Stockholm	-2.8	-3	0.1	-5	-5.3	-2.7	-27	-27	-20	-14.5
New York	0.5	1.8	5.7	-3	-1.9	1.4	-21.1	-26.1	-16.1	-11.1
Frankfurt	1	2	6	-1	-1	2	-20	-18	-12	-8.3
Lausanne	1.3	2.8	5.5	-0.5	0.5	2.7	-9.7	-13	-9.1	-4.9
Brussels	3.3	3.7	6.8	0.7	0.7	3.1	-17	-13	-7	-5.4
London	4.3	4.5	6.9	1.2	1	2.8	-12	-13	-7	-4.5
Paris	5	5.6	8.8	2.7	2.8	5.3	-14.6	-14.7	-9.1	-4.6
Seattle	5.6	6.3	8.1	2.7	2.7	4.1	-22.8	-27.4	-15	-9.3

performance of a heating system is closely tied to its norm outside temperature and the resulting design heat load. A climate region with a larger variance in the outside temperature requires a more powerful heating system to cope with the lowest temperatures. This "excess capacity" to deal with the norm outside temperature (cf. Section 4.2) then also reduces the ramp-up time during warmer days. Table 6 shows the average, average lowest and absolute lowest outside temperatures for the months from January to March for a selection of cities around the world. Since we were missing detailed weather data for the last 20 years for all cities, the norm outside temperature was determined as the mean of the average lowest and the absolute lowest temperatures from January to March.

The table shows that Toronto has the largest differences between the monthly average temperatures and the norm outside temperature Θ_d (varying from 13 °C to 18 °C), while Beijing has the lowest (between 5 °C and 15 °C). A heating system in Toronto is thus designed for a temperature of −19 °C, while a heating system in Beijing is sized to match outside temperatures around −9 °C.

We have used these data to simulate the impact of different climate scenarios by creating, for each city, three weather scenarios with constant temperatures equaling the average temperatures during the months from January to March. This means, for example, that the month of January in Toronto was simulated using a constant temperature of −5.8 °C. All weather scenarios were modelled without solar gains.

4 Building configurations

Our goal is to build a simulation framework that allows to show bounds on the potential of occupancy prediction algorithms to save energy in domestic heating scenarios. In the simplest case, the possible savings are determined by the insulation of the building (transmission losses), its orientation and number of windows (solar gains), the building's exposure and tightness (ventilation losses) as well as heat gains due to occupants and appliances (internal gains). In the following section, we will describe how we calculated these heat losses and gains for four fictitious building scenarios.

In reality, the extend of the possible energy savings in a heating scenario is also dependent upon many other factors. Besides the particular solar energy transmittance of the glass used, solar gains are also influenced by the level of shading afforded by blinds, overhangs and other buildings or structures. Furthermore, the potential for solar gains is highly dependent on the location of the building. In mountainous terrain such as Switzerland, the sun may be partly or completely obscured during large parts of the day, resulting in lower solar gains. Similarly, ventilation losses are influenced not only by the characteristics of the building itself but also by its surroundings. An exposed building has higher ventilation losses than a building that is shielded off by adjacent structures. In addition to the tightness of the building, the level of exposure in conjunction with the current wind conditions determines the amount of ventilation losses. For similar reasons, the amount of heat losses due to ventilation is dependent on the height of the building. For tall buildings, the wind conditions near the top are different to those near ground level.

Unless the building is detached and completely exposed, the energy required to heat might also vary as neighbouring buildings contribute to either transmission gains or losses. In particular, in an apartment complex, a particular party might not need to heat at all if the adjacent parties have heated their apartments to temperatures exceeding the comfort temperature of the first party. In fact, the heating scenario becomes much more complicated when multiple zones with different setpoint temperatures, unconditioned zones and occupancy schedules are considered. In this report we focus on an idealised scenario in which there is no heat transmission from and to adjacent buildings or zones. The buildings are considered to be a single zone with a single temperature setpoint. This simplification allows us to isolate the effect of the occupancy prediction algorithms on the energy expenditure of the building. We leave the analysis of the savings potential inherent in occupancy schedules of multi-party buildings to future work.

The two building configurations used in this study are a studio flat and a house. Both were simulated with low U-values following recent legislatorial guidelines [1] (good insulation: F-U$_{low}$ and H-U$_{low}$) and high U-values (bad insulation: F-U$_{high}$, H-U$_{high}$), respectively. We then expose each of these four fictitious properties to a range of environmental conditions. Figures 4 and 5 show the geometry of the two simulated properties. The studio flat (F-U$_{low}$ and F-U$_{high}$) has an area of 52m^2. The house (H-U$_{low}$ and H-U$_{high}$) has an area of 176m^2. All windows are sized 1.4m by 1.4m. The height of the rooms is 2.5m in both cases. The doors are 1.4m by 2m. The flat has one window facing east, and 3 windows facing south. The house has two east-facing windows, four windows on the south side, two to the west and two windows facing north.

In the remainder of this section, we will show how we calculated the available heating power $\Phi_{H,max}$ (design heat load) as well as the heat gains (Φ_{int} and Φ_{sol}) and heat transfer coefficients for the ISO 13790 5R1C model ($H_{tr,w}$, $H_{tr,op}$ and H_{ve}). Table 7 summarises the resulting parameters used in the simulation using the ISO 13790 5R1C model.

Table 7. 5R1C model parameters for different building variants.

	Building variant				
Parameter	**F-U$_{\text{low}}$**	**F-U$_{\text{high}}$**	**H-U$_{\text{low}}$**	**H-U$_{\text{high}}$**	**Units**
Thermal transmission coefficient for opaque building elements – $H_{tr,op}$	47.16	184.57	103.57	379.35	W/K
Thermal transmission coefficient for windows and doors – $H_{tr,w}$	12.68	31.50	33.07	102.06	W/K
Thermal transmission coefficient for ventilation – H_{ve}	47.33	47.33	161.57	161.57	W/K
Internal zone capacitance – C_m	8.51	8.51	29.04	29.04	MJ/K
Floor area – A_f	51.56	51.56	176.00	176.00	m^2
Design heat load according to [4] – $\Phi_{H,max}$	2.80	6.86	7.78	16.75	kW

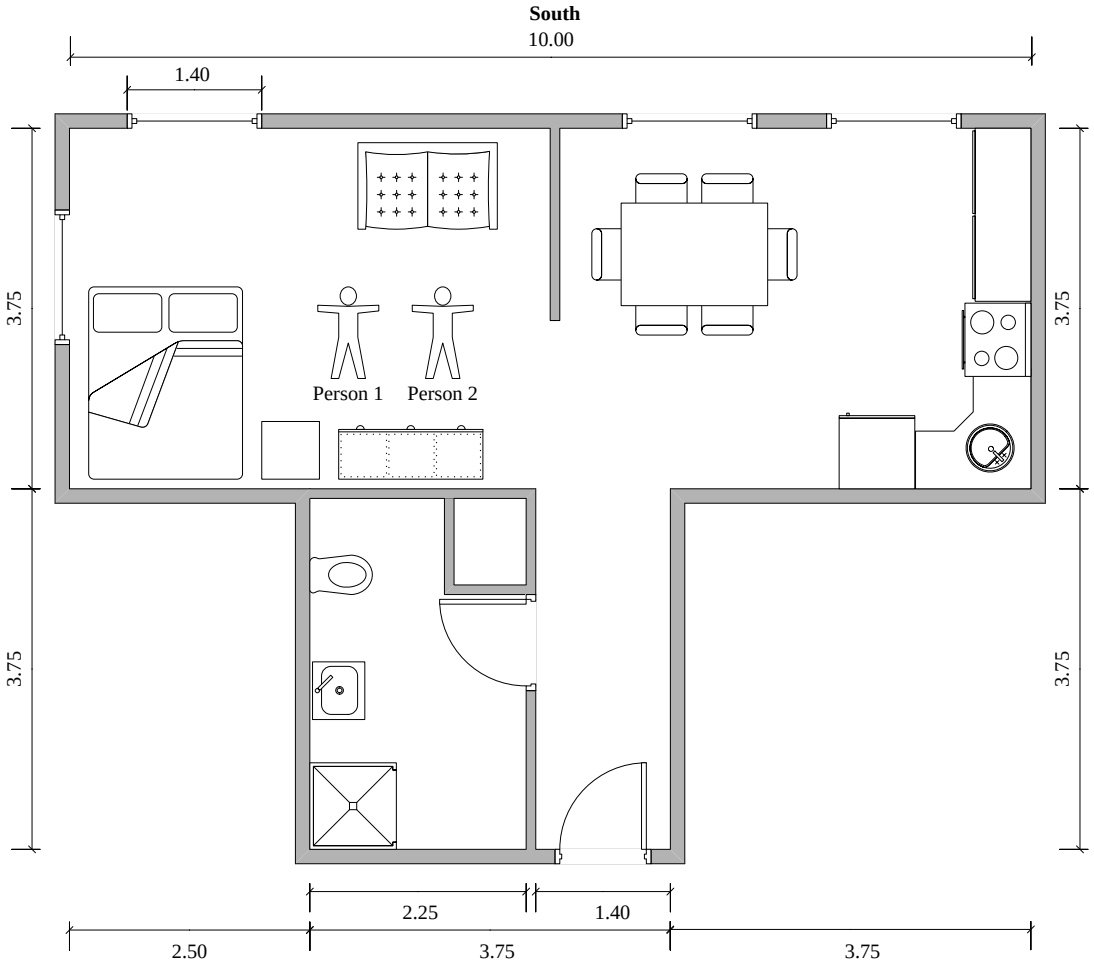

Fig. 4. Blueprint of studio flat (F-U$_{low}$ and F-U$_{high}$).

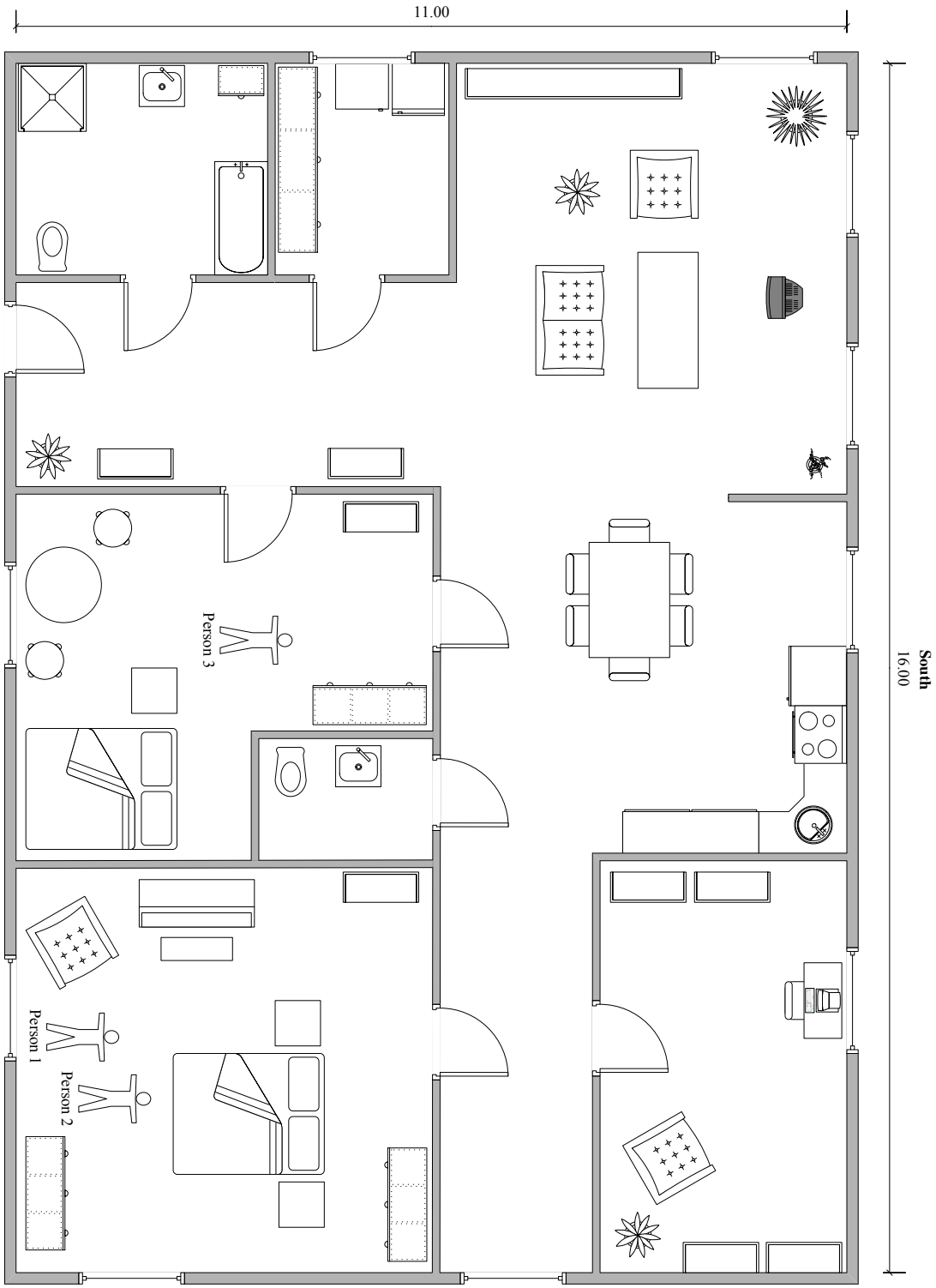

Fig. 5. Blueprint of house (H-U$_{low}$ and H-U$_{high}$).

4.1 Transmission losses – $H_{tr,w}$ and $H_{tr,op}$

A large share of the heat lost during cold weather is due to insufficient insulation. The insulation capacity of a material is described using the so-called U-value. The U-value gives the amount of energy (J) which is transmitted across the component at every second for a certain difference in temperature (K). As the difference between the inside and outside temperatures increases, the building loses more energy to its surroundings. The U-value is the inverse of the R-value with SI units of $W/(m^2K)$. Table 8 shows two sets of characteristic U-values. The first set is taken from a low U-value reference building [1]. As there is no standard definition of high U-values (often anything higher than current building regulations allow is considered high), we have taken generic high U-values from `wikipedia.org`[4] for the low insulation case.

Table 8. U-values ($W/(m^2K)$).

Component	Low U-Values (EnEv 2014)	Generic high U-Values
Walls, ceiling against outside	0.28	1.5
Ground plate	0.35	1.0
Roof	0.20	1.0
Windows	1.30	4.3
Doors	1.80	1.8

The heat transfer coefficients $H_{tr,w}$ and $H_{tr,op}$ are calculated by multiplying the surface area of the building part facing the outside with its U-value.

$$H_{tr,w} = \boldsymbol{A_{walls,ceiling}} \cdot (\boldsymbol{U_{walls,ceiling}} + \boldsymbol{\Delta U_{WB}}) + H_{T,g}$$
$$H_{tr,op} = \boldsymbol{A_{doors,windows}} \cdot (\boldsymbol{U_{doors,windows}} + \boldsymbol{\Delta U_{WB}})$$

where ΔU_{WB} is a generic thermal bridge correction factor which is set to 0.05 according to [9]. The calculation of the heat transfer coefficient to the ground $H_{T,g}$ is shown in the next section.

4.2 Design heat load – $\Phi_{H,max}$

In order to appropriately dimension the heating infrastructure (e.g. radiators and boilers) in a property, the DIN EN 12831 standard allows for the calculation of the design heating load. The design heating load is the amount of heat that needs to be supplied to a building to keep the target comfort temperature Θ_{int} even when the outside temperature is at its lowest. In the case of the DIN EN 12831 model, Θ_d, the design outside temperature, is the lowest two-day average temperature which was measured at least 10 times over a period of 20 years. We have determined Θ_d using meteorological data from MeteoSwiss. Θ_d was calculated to be $-6\,^\circ$C for the period from Jan 1994 to Jan 2014 for Pully, Switzerland. Likewise, we determined the yearly mean of the outside temperature $\Theta_{m,e}$ to be $11.3\,^\circ$C. The temperature variable used for the calculations was the 10-minute average temperature (2m above ground). The target indoor temperature Θ_{int} was $20\,^\circ$C. The resulting design heat loads are shown in Table 9. They are within the range of buildings built from 1978 to 1983 (high U-values) and buildings built after 2001 (low U-values) [7].

Table 9. Design heat load for each building variant.

	Building variant				
Term	**F-U$_{low}$**	**F-U$_{high}$**	**H-U$_{low}$**	**H-U$_{high}$**	**Units**
$\Phi_{H,max}$	2.80	6.86	7.78	16.75	kW
$\Phi_{H,max}$ per m^2	12	30	10	21	W/m^2

[4] `en.wikipedia.org/wiki/Thermal_transmittance`

Table 10. DIN EN 12831 [4] parameters. † DIN EN 12831 refers to the norm outside temperature by Θ_e. To avoid confusion with the current outside temperature Θ_e as defined in ISO 13790, we chose to rename it.

Symbol	Units	Description
$\Phi_{H,max}$	W	Design heat load: $\Phi_{TL} + \Phi_V$
Φ_{TL}	W	Heat loss due to transmission
Φ_V	W	Heat loss due to ventilation
$H_{T,e}$	K/W	Heat transmission coefficient to the outside (R-value)
$H_{T,g}$	K/W	Heat transmission coefficient to the ground (R-value)
Θ_{int}	K	Indoor temperature
Θ_d †	K	Norm outside temperature
$\Theta_{m,e}$	K	Yearly mean of outside temperature
A_f	m^2	Floor area
P	m	Circumference of ground plate in contact with environment

Heat transmission coefficients The heat loss due to ventilation Φ_V was calculated using the method used in Section 4.3 to determine the heat transfer coefficient for the ventilation H_{ve}. The heat *transmission coefficient to the ground* $H_{T,ig}$ was calculated using the method from [9]:

$$H_{T,g} = A_f \times U_{equiv} \times f_{g1} \times f_{g2}$$

where $f_{g1} = 1.45$, $f_{g2} = (\Theta_{int,i} - \Theta_{m,e})/(\Theta_{int,i} - \Theta_e)$ and U_{equiv} from Table 11 using $B' = \frac{A_g}{2P}$. The heat *transmission coefficient to the outside* was calculated as:

$$H_{T,e} = \boldsymbol{A} \cdot (\boldsymbol{U} + \boldsymbol{\Delta U_{WB}})$$

where A and U are vectors containing the areas and U-values of the buildings parts' (i.e. walls, windows, doors and ceiling), respectively. ΔU_{WB} is a generic thermal bridge correction factor which is set to 0.05 according to [9]. The U-values used for the calculation of $H_{T,g}$ and $H_{T,e}$ are the same as used in the previous section (cf. Table 8).

Table 11. Equivalent transmission coefficient U_{equiv} for buildings without cellar. Table from [9].

B'[m]	U_{equiv} $[W/(m^2K)]$				
	$U_{ground\ plate}$ $[W/(m^2K)]$				
	no insulation	2.0	1.0	0.5	0.25
2	1.30	0.77	0.55	0.33	0.17
4	0.88	0.59	0.45	0.30	0.17
6	0.68	0.48	0.38	0.27	0.17
8	0.55	0.41	0.33	0.25	0.16
10	0.47	0.36	0.30	0.23	0.15
12	0.41	0.32	0.27	0.21	0.14
14	0.37	0.29	0.24	0.19	0.14
16	0.33	0.26	0.22	0.18	0.13
18	0.31	0.24	0.21	0.17	0.12
20	0.28	0.22	0.19	0.16	0.12

4.3 Ventilation losses – H_{ve}

Ventilation heat losses occur due to cracks or small openings in the building envelope (natural ventilation) and the need to regularly exchange the air to increase the comfort of the inhabitants (hygienic ventilation). In the following section, we will discuss how we calculated the ventilation heat losses according to the DIN EN 12831 model.

Natural ventilation mainly depends on the tightness of the building envelope, the exposure of the building and the wind speed. Some of the heat losses from natural ventilation may be thus recovered by making windows and doors draught-proof. On the other hand, heat losses due to hygienic ventilation arise from the need for inhabited spaces to be regularly ventilated to reduce the concentration of harmful gases such as carbon dioxide. Ventilation is also necessary to counter the humidity introduced by inhabitants (e.g. by breathing, cooking or taking a shower) – which may lead to mold. Therefore these losses cannot be avoided. The *Recknagel*[5] [20] minimum (hygienic) ventilation is defined as the minimum amount of air exchange required to maintain 1000 ppm CO_2.

For our model, we have calculated the heat losses due to ventilation H_{ve} using the simplified method from DIN EN 12831. In DIN EN 12831, H_{ve} is defined as the maximum of the hygienic minimum ventilation V_{min} and V_{inf}, the natural ventilation by infiltration. V_{min} is the volume of the room to be heated multiplied by a factor n_{min}. In this case, we chose $n_{min} = 0.5$ which is given by DIN EN 12831 as the standard value for an inhabited room. The heat loss due to infiltration is given by:

$$V_{inf} = 2 \times V_r \times n_{50} \times e \times \epsilon$$

Here V_r denotes for the volume of the room, n_{50} is a factor for the tightness of the building. We set $n_{50} = 6$, which corresponds to a detached house with tight walls. The shielding factor e we set to 0.09 which corresponds to moderate shielding. We do not employ an elevation correction and thus set $\epsilon = 1$. Since $V_{inf} = 2 \times V_r \times 6 \times 0.09 \times 1 = 1.08$, $V_{inf} > V_{min}$, which means that the hygienic air flow is already guaranteed by the natural ventilation, $H_{ve} = V_{inf}$. The ventilation heat transfer coefficient is thus equivalent to the losses due to natural ventilation.

4.4 Internal gains – $\boldsymbol{\Phi_{int}}$

Internal heat gains are divided into gains due to *appliances* (e.g. dishwasher, washing machine, dryer and stove), *losses from the heating/cooling system* (e.g. pumps and fans) and the *metabolic heat from occupants*. We do not include internal gains due to appliances since we do not have accurate ground truth data to predict their operation. In addition, we assume that there are no losses from the heating system that may be recovered as part of the internal gains. We do, however, include internal gains due to the metabolic heat rate of the occupants. An average person produces 125 W of heat [12]. For our simulation we have assumed the flat to be occupied by 2 people and the house by 3 people. Since the algorithms in our sample only consider binary occupancy, we assumed all occupants to be present whenever the property was occupied (i.e. $\Phi_{int} = 250W$ and $\Phi_{int} = 375W$ whenever the flat or house are occupied, respectively).

4.5 Solar gains – $\boldsymbol{\Phi_{sol}}$

While solar gains are most important when assessing the need for air-conditioning and ventilation in summer, the sun's radiation must also be taken into account to properly assess the energy needed for heating in winter. Such is the importance of solar gains that the field of passive solar building design focuses on using solar gains in winter and avoiding those gains in summer through the placement of windows, shading and insulation [19].

An increase in temperature through solar gains is the net result from two different processes: (a) long wavelength radiation being trapped inside the building and (b) an increase in the temperature of the building envelope through absorbed sunlight. In this report we will focus on the former – solar gain through transparent building parts. When a building material such as glass is more transparent to the shorter wavelengths (visible light) than the longer (infrared radiation), heat is trapped inside the room. This is due to the fact that the room is heated up and any re-emitted (infrared) radiation cannot escape through the windows. This effect is best exhibited in green houses and occurs at a smaller scale in residential buildings.

[5] The *Taschenbuch für Heizung + Klimatechnik* or *Recknagel* in short is the standard reference for heating and cooling in the German language. First issued in 1897, it is currently in its 76th issue.

The incident solar radiation causing the internal gains may be divided into two categories: Direct and diffuse radiation. Direct radiation are direct line-of-sight rays from the sun, while diffuse radiation is light reflected from the surroundings. The direct radiation is the reason why, in the northern hemisphere, buildings are often constructed with windows facing south to maximise exposure to the sun.

The weather data used in the following experiments contains the global (direct + diffuse) radiation on a horizontal surface. To calculate the solar gain through the windows, we must first obtain the position of the sun relative to our location. We then divide the global radiation into direct and diffuse radiation using the Reindl* method [10]. Finally, we transform the direct radiation from the horizontal to a vertical plane and thence to the different orientations of the windows.

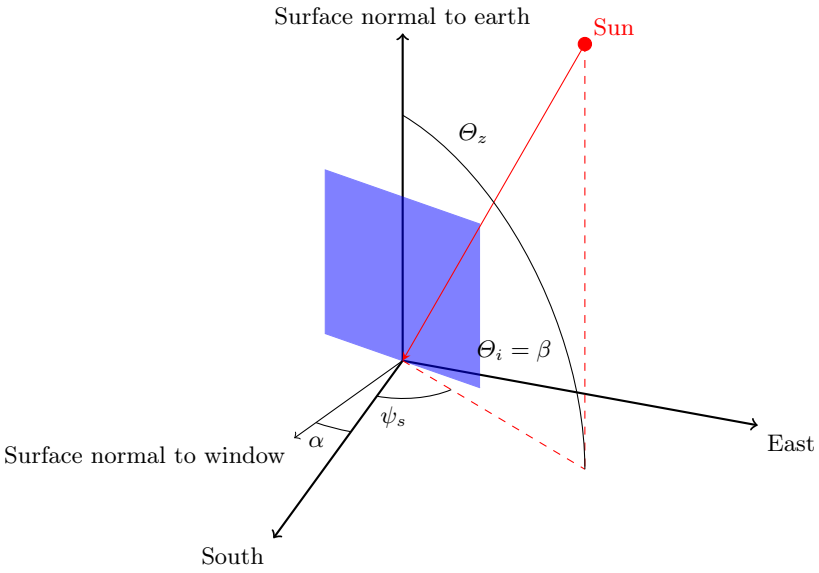

Fig. 6. Position of the sun. Θ_z is the solar zenith angle. Θ_i is the angle between the normal to the window and the sun. In our case the normal to the surface of the window is assumed to be perpendicular to the normal to the surface of the earth and therefore β, the solar elevation is $\beta = 90 - \Theta_z = \Theta_i$. α is the orientation of the window with 0 degrees being south.

Position of the sun In order to correctly compute the incident solar radiation on the windows, we must find the sun's current position in terms of its elevation β and azimuth angle ψ_s. The sun's elevation is at its maximum over noon. Figure 6 shows a simplified version of the problem. In this case the normal to the surface of the window is assumed to be perpendicular to the normal to the surface of the earth (i.e. there is no tilt or rotation of the window in the vertical plane).

β and ψ_s are calculated as follows:

$$\sin\beta = \cos lat \cos\delta \cos\omega + \sin lat \sin\delta$$

$$\sin\psi_s = \cos\delta \frac{\sin\omega}{\cos\beta}$$

The calculation of β and ψ_s needs the local apparent solar time of the current position. This is due to the fact that the Earth follows an elliptical orbit and that its axis is not perpendicular to the plane of that orbit. The result is that the mean solar time (clock time) does not accurately reflect the current position of the sun. The local apparent solar time *suntime* is calculated as follows using the variables defined in Table 13:

Table 12. Sun angle parameters.

Variable	Description
lat	latitude of building
δ	$23.45 \sin(284+n)\frac{360}{365}$, where n = day of the year
ω	$0.25(suntime - 720)$

$$suntime = time + 4(lat - lat_{st}) + E$$

Table 13. Parameters for the calculation of the local apparent solar time.

Variable	Description
$time$	local time (CET)
lon	longitude of building
lon_{st}	standard meridian of building / CET (15)
$4(lat - lat_{st})$	constant deviation (4 minutes per degree)
E	$9.87 \sin 2B - 7.53 \cos B - 1.5 \sin B$
B	$(n-81) * 360/364$, where n = day of the year

Direct and diffuse radiation: Reindl* With the current elevation β of the sun, we can split the global radiation obtained from the weather data into direct and diffuse components. As the Pully station does not provide detailed information on the cloud cover including the type of clouds, position and number of layers, we must use a decomposition model to determine incident direct and diffuse radiation [10]. The Reindl* is a piecewise regression to compute the relationship between the diffuse radiation I_d and the global radiation I with respect to a clearness factor k_t. The clearness factor depends on the extraterrestrial radiation (solar energy) I_0, the current global radiation I as measured by the weather station as well as Θ_z, the angle between the zenith and the sun. The method is described in detail in [10]. The parameters are listed in Table 14.

$$I_d/I = \begin{cases} 1.020 - 0.248k_t & \text{if } 0 \leq k_t \leq 0.3, I_d/I \leq 1.0 \\ 1.400 - 1.749k_t + 0.177 \sin\beta & \text{if } 0.3 < k_t < 0.78, 0.1 \leq I_d/I \leq 0.97 \\ 0.147 & \text{if } k_t \leq 0.78 \end{cases}$$

Table 14. Reindl* parameters.

Variable	Description
I	Global radiation as measured by the weather station
I_d	Diffuse radiation on the horizontal surface
I_b	Direct radiation on the horizontal surface
I_0	Extraterrestrial radiation / solar energy in W/m^2
I_0	$1356.5 + 48.5 \cos(0.01721 * (n-15))$
k_t	$\frac{I}{I_0 \cos\Theta_z}$, Clearness factor $0 \leq k_t \leq 1$
Θ_z	$90 - \beta$, angle between zenith and sun

4.6 Solar radiation on vertical surfaces

From the incident direct solar radiation on the vertical plane, we can now compute the direct solar radiation on a vertical plane using the angles computed previously as follows:

$$I_{b,vert} = \frac{I_b}{\cos\theta_z}\cos\theta_i$$

where

$$\cos\theta_i = -\sin\delta\cos lat\cos\alpha + \cos\delta\cos lat\cos\alpha\cos\psi_s + \cos\delta\sin\alpha\sin\psi_s$$

Here α is the clockwise orientation of the window with 0 degrees being south (cf. Figure 6). For our model we assume that the house is positioned directly on the the north south axis. This means that that the windows are facing directly to the north, east, south and west directions. In order to calculate the incident solar radiation on the windows we can use the following equation:

$$\Phi_{sol,x} = A_{W,x} \times g(0) \times (1 - \tan^4(\Theta_i/2)) \times \frac{I_b}{\cos\Theta_z} \times \cos\Theta_i$$

Here $A_{W,x}$ is the area of the windows ($x \in \{east, south, west\}$) and g(0) is the g-value (solar transmittance) of the window. We set $g(0) = 0.6$, corresponding to double-glazed windows. I_b and Θ_z are the direct solar radiation on the horizontal plane and the angle between the zenith and the sun as previously calculated. Once we have obtained $\Phi_{sol,east}$, $\Phi_{sol,south}$ and $\Phi_{sol,west}$, Φ_{sol} is computed as the sum of the individual solar gains (i.e. $\Phi_{sol} = \Phi_{sol,east} + \Phi_{sol,south} + \Phi_{sol,west}$). Like the temperature Θ_e, the solar gains Φ_{sol} have been calculated at 15-minute intervals for all[6] $\beta > 5$.

5 Controller design

In order to act upon the predictions made by the occupancy prediction algorithms [8,17,18,21], we must translate their predicted occupancy schedules into an actual heating schedule containing setpoint temperatures. As the heating system cannot reach the target comfort temperature immediately, these setpoint temperatures have to be chosen so to reach a comfortable temperature upon the occupants' arrival (e.g. in order to reach a comfortable temperature upon the arrival of the occupants at 5 p.m. we might have to set the setpoint temperature to the comfort temperature at 3 p.m. already).

Table 15. Controller parameters.

Symbol	Units	Description
$\Theta_{comfort}$	°C	Comfort / set-point temperature
$\Theta_{setback}$	°C	Setback temperature
t	/	Current 15-minute timeslot
S	$\{1,0\}$	Actual occupancy schedule
P_t	$\{1,0\}$	Predicted occupancy schedule at interval t

Algorithm 1 shows the high-level[7] controller used to alternate between setpoint $\Theta_{comfort}$ and setback $\Theta_{setback}$ temperatures. The rationale behind our approach is that by simulating the time it takes to heat up the property to a comfortable temperature, we can decide if the predicted schedule gives us enough time to forgo heating for another timestep. For each 15-minute time interval t, the controller looks at the current occupancy S_t of the household given by the occupancy schedule S at at time t. If the household is currently occupied, we must keep the setpoint temperature and therefore we set $\Theta_{int,H,set}$ to $\Theta_{comfort}$. If the household is not occupied at time t, we use the predictive policy. The predictive policy first looks at the current prediction from time t onwards P_t and finds the number of intervals until the next occupied interval. It then computes the next indoor temperature $\Theta_{air,noheat}$, which would result from using the setback temperature for the current

[6] The clearness factor k_t is only defined for $\beta > 5$ due to the cosine in $k_t = \frac{I}{I_0 \cos\Theta_z}$.

[7] Further to this, there is an internal controller inside the RC model that regulates the heat input to obtain the desired target temperature at each timestep.

interval. Finally, it computes the number of intervals it will take to heat from $\Theta_{air,noheat}$ to the setpoint temperature $\Theta_{comfort}$. If this number is larger than the number of intervals to the next occupied timeslot, we must heat at the current time t.

A reactive policy is obtained if for all times t_1 and all predicted intervals t_2 at these times, the building is predicted to be unoccupied – or more formally: $\forall t_1, t_2 : P_{t_1,t_2} = 0$. Similarly, an always-on policy is obtained if for all times t during the simulation the building's occupancy is set to 1 – formally $\forall t : S_t = 1$. In the appendix (Section 7), we show the behaviour of the control algorithm for all weather scenarios for a building unoccupied from 9 a.m. to 5 p.m. in terms of the heating setpoint $\Theta_{int,H,set}$ and indoor air Θ_{air} temperatures as well as the heat input – $\Phi_{HC,nd}$.

Algorithm 1 Control algorithm.

procedure CONTROLLER
  $t \leftarrow$ Current time interval
  $S \leftarrow$ Actual occupancy schedule
  $P_t \leftarrow$ Predicted occupancy schedule at interval t
  Reactive policy:
  if isOccupied(S_t) **then**
    $\Theta_{int,H,set} \leftarrow \Theta_{comfort}$
  else
    Predictive policy:
    $n_{horizon} \leftarrow nextOccupied(P_t)$
    $\Theta_{air,noheat} \leftarrow iso13790_{5R1C}(\Theta_{setback}, \Theta_{m,t-1}, \dots)$
    $n_{preheat} \leftarrow$ Preheat time from $\Theta_{air,noheat}$ to $\Theta_{comfort}$
    if $n_{horizon} \geq n_{preheat}$ **then**
      $\Theta_{int,H,set} \leftarrow \Theta_{setback}$
    else
      $\Theta_{int,H,set} \leftarrow \Theta_{comfort}$
  $\Theta_{m,t}, \Phi_{HC,nd,t}, \Theta_{air,t} \leftarrow iso13790_{5R1C}(\Theta_{int,H,set}, \Theta_{m,t-1}, \dots)$.
  $t \leftarrow t + 1$
  goto *Reactive policy.*

5.1 Steady-state

When we first start the simulation, we do not know the value for $\Theta_{m,0}$. As Θ_m – the temperature of the building mass – is different from the indoor air temperature Θ_{air} (cf. Figure 2), we cannot set $\Theta_{m,0} = \Theta_{setback}$. We thus first obtain a steady state temperature for $\Theta_{m,0}$ by repeatedly running `iso13790`$_{5R1C}$`(` $\Theta_{setback}$`,` $\Theta_{m,t-1}$`, ...)` with the same environmental parameters until $\Theta_{m,t}$ converges. For the initial value of $\Theta_{m,t}$ we use $\Theta_{m,setback}$.

6 Limitations of the ISO 13790 5R1C model

Figures 8 to 23 from the appendix show the response of the controller to different weather and building scenarios. In all scenarios, there is a sudden drop in Θ_{air} when the heating is switched off and a notable increase when the heating is turned back on. In this section, we will investigate this effect by examining parameters of the ISO 5R1C model. Figure 7 shows the temperatures[8] simulated by the ISO 5R1C model for a building occupied from midnight to 9 a.m. and again from 5 p.m. to midnight (well insulated flat). The heating setpoint temperature $\Theta_{int,H,set}$ is lowered to the setback temperature at 9 a.m. ($\Theta_{setb} = 10\,^{\circ}\mathrm{C}$) in order to save energy. To reach a comfortable

[8] That is the mean air temperature, Θ_{air}, the mean radiant temperature Θ_m, the heating setpoint temperature $\Theta_{int,H,set}$, the temperature of the surface node Θ_s and the mean operating temperature Θ_{op} (cf. Table 2).

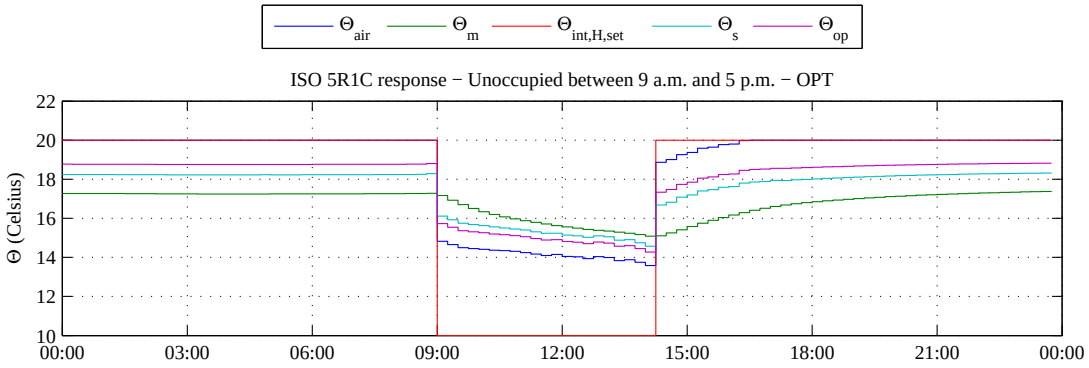

Fig. 7. Temperature response of ISO 5R1C model.

Table 16. Example parameters for the calculation of Θ_{air}.

	Building variant				
Term	**F-U$_{low}$**	**F-U$_{high}$**	**H-U$_{low}$**	**H-U$_{high}$**	**Units**
$H_{tr,is}\Theta_s$ (Heat recovered from surface node)					
$H_{tr,is}$	1044	1044	3564	3564	W/K
$H_{tr,is} \times 16\,°C$	16.70	16.70	57.02	57.02	kW
$H_{tr,is} \times 18\,°C$	18.79	18.79	64.15	64.15	kW
$H_{ve}\Theta_{sup}$ (Heat loss by ventilation)					
H_{ve}	47.33	47.33	161.57	161.57	W/K
$H_{ve} \times 0\,°C$	0	0	0	0	kW
$H_{ve} \times -5\,°C$	-0.24	-0.24	-0.81	-0.81	kW
$H_{ve}\Theta_{sup}$ (Maximal heat gains when occupied)					
Φ_{ia}	0.13	0.13	0.19	0.19	kW
$\Phi_{HC,nd}$ ($\Phi_{H,max}$)	2.80	6.86	7.78	16.75	kW

temperature (i.e. $\Theta_{air} = \Theta_{comf}$) upon the arrival of the occupants, $\Theta_{int,H,set}$ is set to the comfort temperature ($\Theta_{comf} = 20\,°C$) at 2.15 p.m. – this "optimal" control strategy is described in more detail in Section 5.

The development of the indoor air temperature Θ_{air} in Figure 7 is noteworthy. As the heat input from the heating system is reduced to zero at 9 a.m., Θ_{air} drops by over 5 °C. Similarly, there is a significant jump in Θ_{air} when the heat input is increased again at 2.15 p.m.. The circuit diagram in Figure 2 shows that the heat source $\Phi_{HC,nd}$ is directly connected to the node for the indoor air temperature Θ_{air}. Θ_{air} loses heat to the outside while heating the supplied air. It further exchanges heat with the building surface. The capacitor C_m, which stores some of the heat is located at the other side of the circuit. While the function for Θ_m is continuous and shows no jumps in the temperature, this arrangement causes the function for Θ_{air} to be discontinuous. This can also be seen from the calculation of Θ_{air} (Eqn. C11, ISO 13790). Here, Θ_{air} is derived from Θ_m via Θ_s:

$$\Theta_{air} = (H_{tr,is}\Theta_s + H_{ve}\Theta_{sup} + \Phi_{ia} + \Phi_{HC,nd})/(H_{tr,is} + H_{ve})$$

Table 16 shows an exemplary calculation of the parameters of the above equation at 9 a.m.. The coupling conductance $H_{tr,is}$ between the air node Θ_{air} and the surface node Θ_s is given by $H_{tr,is} = h_{is}A_{tot}$ where $h_{is} = 3.45$ (see 7.2.2.2 of ISO 13790). A_{tot} is the area of all surfaces facing the building zone and calculated as $A_f \times 4.5$. As $H_{tr,is}$ is fixed for each building configuration, the first term of the summation only varies with Θ_s. When Θ_s is 18 °C (9 a.m.), the heat from the inner surface of the building is 19 kW for the flat and 64 kW for the house. As Θ_s drops to 16 kW after the heating is switched off, this heat is reduced to 17 kW and 57 kW for the flat and house, respectively. In both cases, this is a decrease of 11% in the energy supplied by the walls to heat Θ_{air}

H_{ve} is the ventilation heat transmission coefficient and Θ_{sup} is the temperature of the supplied air – in our case $\Theta_{sup} = \Theta_e$. Thus, the second term only varies with the outside temperature. If we assume that there is no significant difference in the outside temperature between 9 a.m. and 9.15 a.m., this term does not contribute to the steep drop in the indoor air temperature.

Φ_{ia} is defined as half of the internal gains. $\Phi_{HC,nd}$ is the heat input, bounded above by the design heat load. The drop in temperature occurs when the building is unoccupied after 9 a.m. as both $\Phi_{HC,nd}$ and Φ_{ia} become zero[9]. Table 16 shows that Φ_{ia} only contributes 0.13 kW to 1.19 kW to the overall gains. In contrast, the impact from switching off the heating system is much larger. Depending on the level of insulation and the size of the building, between 2.8 kW and 16.75 kW are removed entirely from the system at 9.15 a.m.. Especially for the poorly insulated buildings, the heat supplied directly by the heating system (rather than through the surface node) has a substantial effect on the indoor air temperature. For the poorly insulated flat, the heating system can supply 7 kW, while the walls supply 19 kW at 18 °C and 17 kW at 16 °C. Removing this heat from the system entirely, invariably produces the significant drop in temperature after 9 a.m.

To lengthen the ramp-up time and in order for it to more accurately reflect the heating behaviour of hydronic heating systems common in Europe, the 5R1C model should be extended to model the lag caused by boilers and radiators. A hydronic heating system needs to heat up the water in circulation first, before the heat can be transmitted to the indoor air and the structure of the building via radiation. Similarly, the temperature in the radiators does not drop immediately when the setpoint temperature is lowered. Pipes, radiators and the boiler may thus constitute an additional RC circuit, separated from the rest of the building.

7 Summary

In this report we have presented a predictive controller and a method for calculating the energy consumption induced by heating a building based on the ISO 13790 5R1C model. In order to assess the effect of different building characteristics, we have modelled a flat and a house, both with poor and good insulation levels. We have furthermore investigated the effect of weather and climate conditions by introducing characteristic weather scenarios for the Lausanne area. We have shown how these scenarios can be used to determine the annual energy savings of a smart heating system. We used the modelling framework to analyse a number of smart heating strategies in [16].

References

1. Verordnung über energiesparenden Wärmeschutz und energiesparende Anlagentechnik bei Gebäuden in der Fassung der Bekanntmachung vom 24. Juli 2007 (BGBl I S. 1519), zuletzt geändert am 18. November 2013 (BGBl I S. 3951–3990) (2013)
2. Beuken, C.L.: Wärmeverluste bei periodisch betriebenen elektrischen Öfen: Eine neue Methode zur Vorausbestimmung nicht-stationärer Wärmeströmungen. Ph.D. thesis, Sächsische Bergakademie Freiberg (1936)
3. Corrado, V., Fabrizio, E.: Assessment of building cooling energy need through a quasi-steady state model: Simplified correlation for gain-loss mismatch. Energy and Buildings 39(5), 569–579 (2007)
4. DIN: Heating systems in buildings - method for calculation of the design heat load. DIN EN 12831-03:2008, Deutsches Institut für Normung, Berlin, Germany (2008)
5. Erickson, V., Carreira-Perpiñán, M., Cerpa, A.: OBSERVE: Occupancy-based system for efficient reduction of HVAC energy. In: Proc. IPSN'11. pp. 258–269. IEEE, Chicago, IL, USA (April 2011)
6. European Parliament and the Council of 16: Directive 2002/91/EC of 16 December 2002 on the energy performance of buildings. Official Journal L 001 pp. 65–71 (December 2002)
7. Forum für Energieeffizienz in der Gebäudetechnik e.V.: Leitfaden zum Heizungs-Check nach DIN EN 15378 p. 20 (May 2010)
8. Gupta, M., Intille, S.S., Larson, K.: Adding GPS-control to traditional thermostats: An exploration of potential energy savings and design challenges. In: Proc. Pervasive'09. pp. 1–18. Springer, Nara, Japan (May 2009)

[9] Depending on the setback and outside temperatures, $\Phi_{HC,nd}$ might stay above zero

9. Hayner, M., Ruoff, J., Thiel, D.: Faustformel Gebäudetechnik. Deutsche Verlags-Anstalt, München, Germany (2013)
10. Helbig, N.: Application of the radiosity approach to the radiation balance in complex terrain. Ph.D. thesis, University of Zurich, Zurich, Switzerland (February 2009)
11. Incropera, F.P., Lavine, A.S., DeWitt, D.P.: Fundamentals of heat and mass transfer. Wiley (2011)
12. ISO: Ergonomics of the thermal environment - analytical determination and interpretation of thermal comfort using calculation of the PMV and PPD indices and local thermal comfort criteria. ISO 7730:2005, International Organization for Standardization, Geneva, Switzerland (2005)
13. ISO: Energy performance of buildings - calculation of energy use for space heating and cooling. ISO 13790-1:2008, International Organization for Standardization, Geneva, Switzerland (2008)
14. Jokisalo, J., Kurnitski, J.: Performance of EN ISO 13790 utilisation factor heat demand calculation method in a cold climate. Energy and Buildings 39(2), 236–247 (2007)
15. Kirchner, A., Kemmler, A., Hofer, P., Keller, M., Jakob, M., Catenazzi, G.: Analyse des schweizerischen Energieverbrauchs 2000–2009 nach Verwendungszwecken. Swiss Federal Office of Energy, Bern, Switzerland (December 2010)
16. Kleiminger, W., Mattern, F., Santini, S.: Predicting household occupancy for smart heating control: A comparative performance analysis of state-of-the-art approaches (2014)
17. Lu, J., Sookoor, T., Srinivasan, V., Gao, G., Holben, B., Stankovic, J., Field, E., Whitehouse, K.: The Smart Thermostat: Using occupancy sensors to save energy in homes. In: Proc. SenSys'10. pp. 211–224. ACM, Zurich, Switzerland (November 2010)
18. Mozer, M.C., Vidmar, L., Dodier, R.H.: The Neurothermostat: Predictive optimal control of residential heating systems. In: Mozer, M.C., Jordan, M.I., Petsche, T. (eds.) Advances in Neural Information Processing Systems. vol. 9, pp. 953–959. The MIT Press (1997)
19. Norton, B.: Harnessing Solar Heat. Springer (2014)
20. Recknagel, H., Ginsberg, O., Gehrenbeck, K., Sprenger, E., Hönmann, W., Schramek, E.R. (eds.): Taschenbuch für Heizung + Klimatechnik. Oldenbourg Industrieverlag, München, Germany (2013)
21. Scott, J., Brush, A.J., Krumm, J., Meyers, B., Hazas, M., Hodges, S., Villar, N.: Preheat: Controlling home heating using occupancy prediction. In: Proc. UbiComp'11. pp. 281–290. ACM, Beijing, PRC (2011)

Appendix

Figures 8 to 23 of this appendix show the data used for each of the 8 weather scenarios defined in Section 3 (i.e. temperature $\in \{\text{very low}, \text{freezing}, \text{low}, \text{moderate}\}$ and solar gains $\in \{\text{clear}, \text{cloudy}\}$). The figures also show the response of the predictive controller introduced in Section 5 for an unoccupied period from 9 a.m. to 5 p.m. for all 32 simulated weather and building (i.e. building $\in \{\text{F-U}_{low}, \text{F-U}_{high}, \text{H-U}_{low}, \text{H-U}_{high}\}$) scenarios. The temperature curve generated by the ISO 5R1C model is discussed in more detail in Section 6.

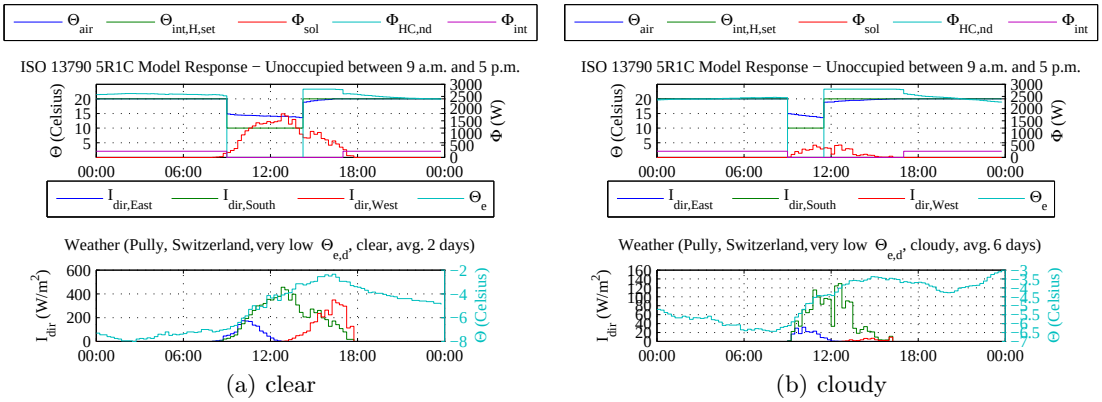

(a) clear (b) cloudy

Fig. 8. ISO 13790 response: Very low temperature, F-U$_{low}$.

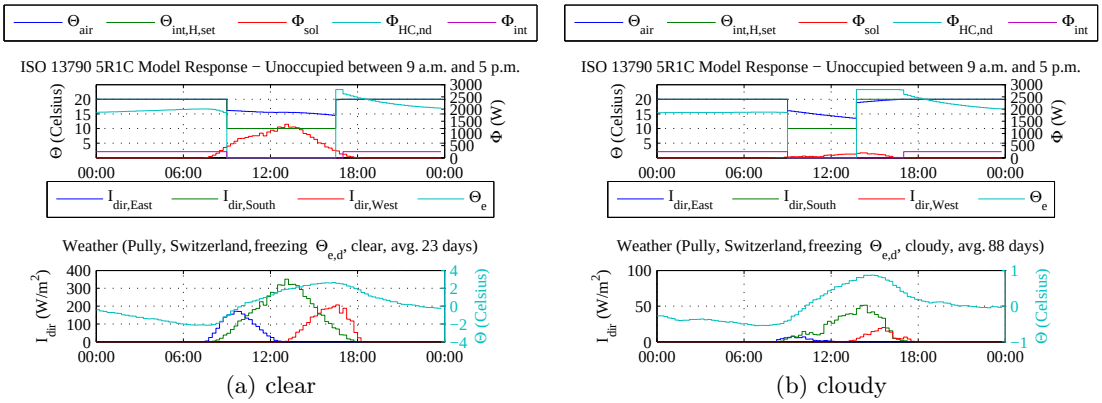

(a) clear (b) cloudy

Fig. 9. ISO 13790 response: Freezing temperature, F-U$_{low}$.

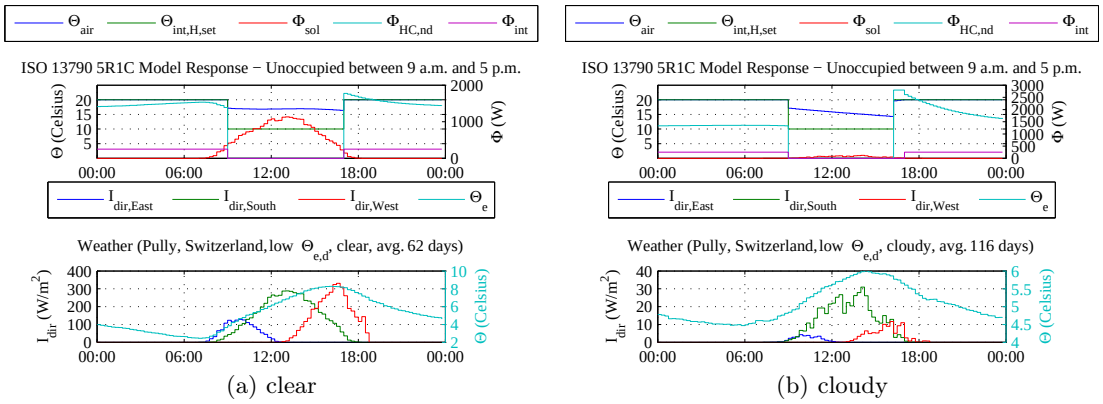

Fig. 10. ISO 13790 response: Low temperature, F-U$_{low}$.

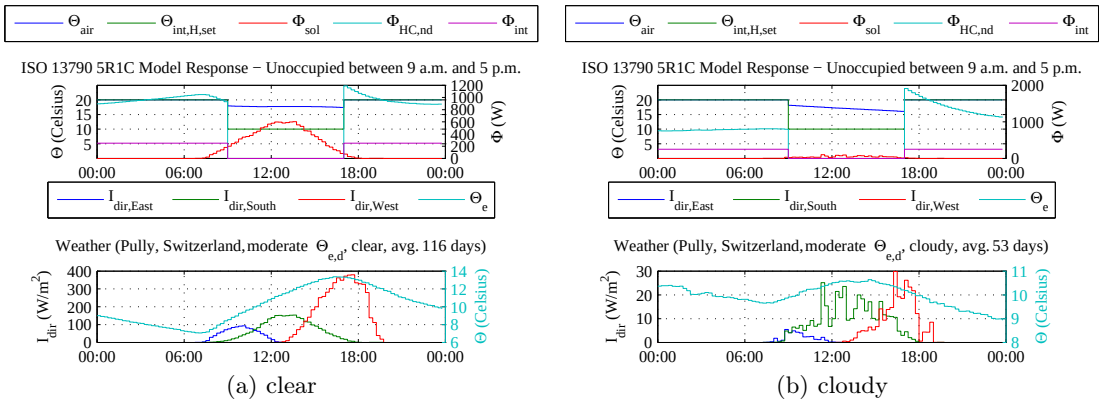

Fig. 11. ISO 13790 response: Moderate temperature, F-U$_{low}$.

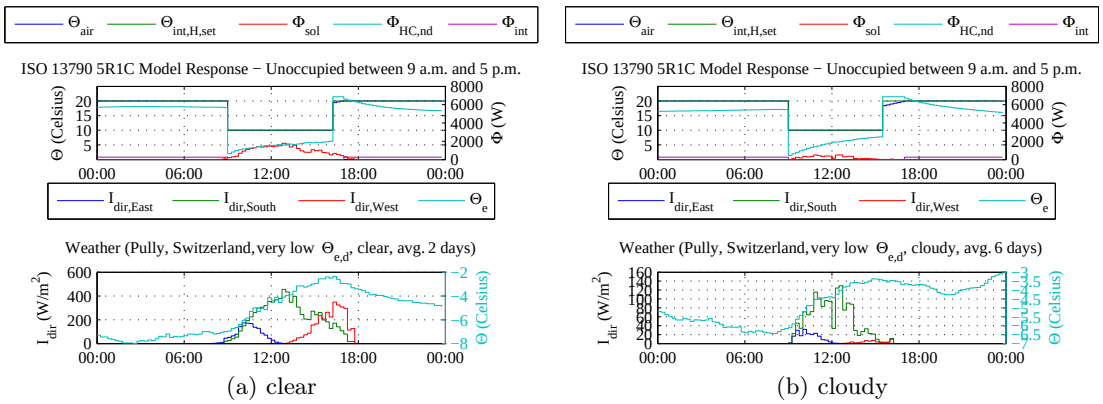

Fig. 12. ISO 13790 response: Very low temperature, F-U$_{high}$.

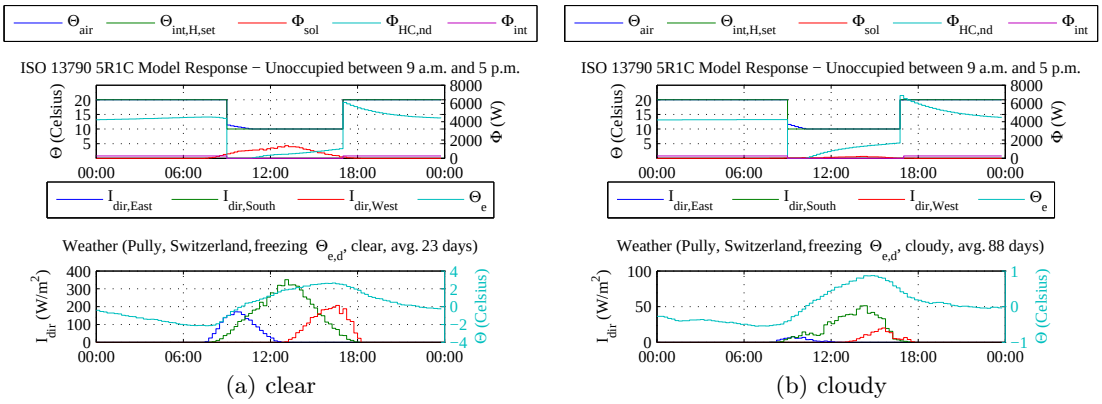

(a) clear (b) cloudy

Fig. 13. ISO 13790 response: Freezing temperature, F-U$_{high}$.

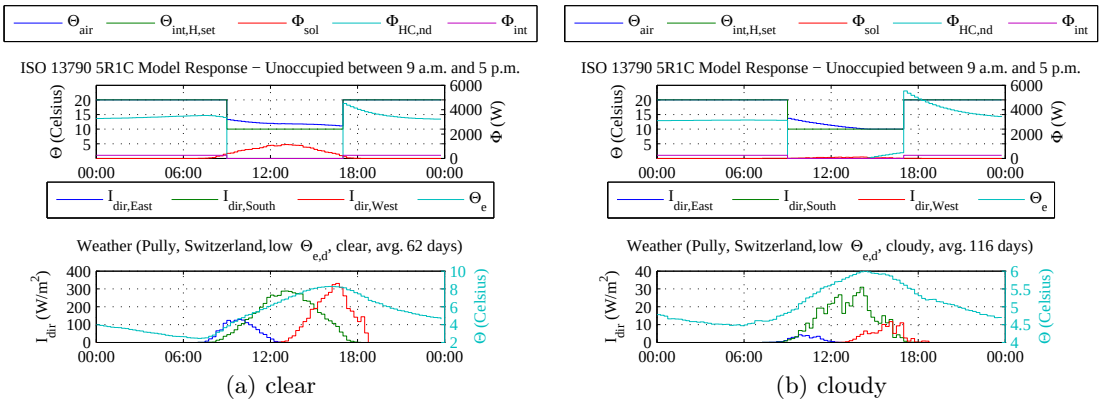

(a) clear (b) cloudy

Fig. 14. ISO 13790 response: Low temperature, F-U$_{high}$.

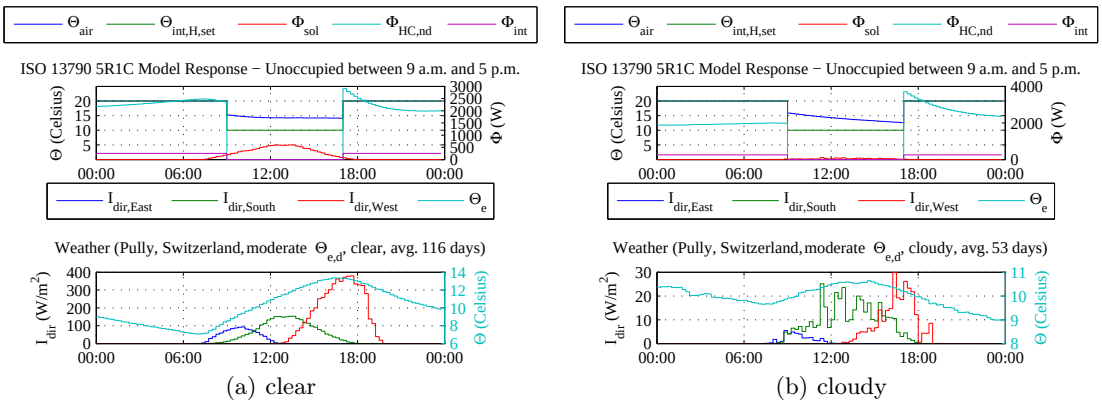

(a) clear (b) cloudy

Fig. 15. ISO 13790 response: Moderate temperature, F-U$_{high}$.

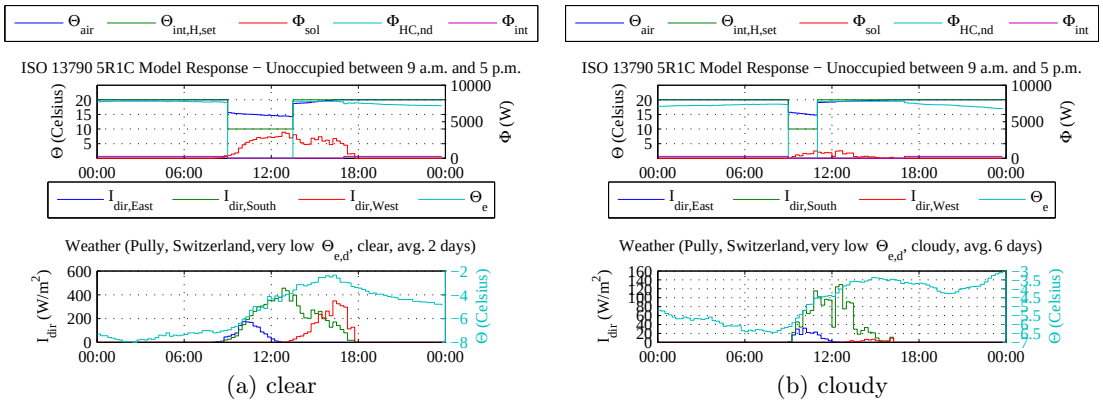

Fig. 16. ISO 13790 response: Very low temperature, H-U$_{low}$.

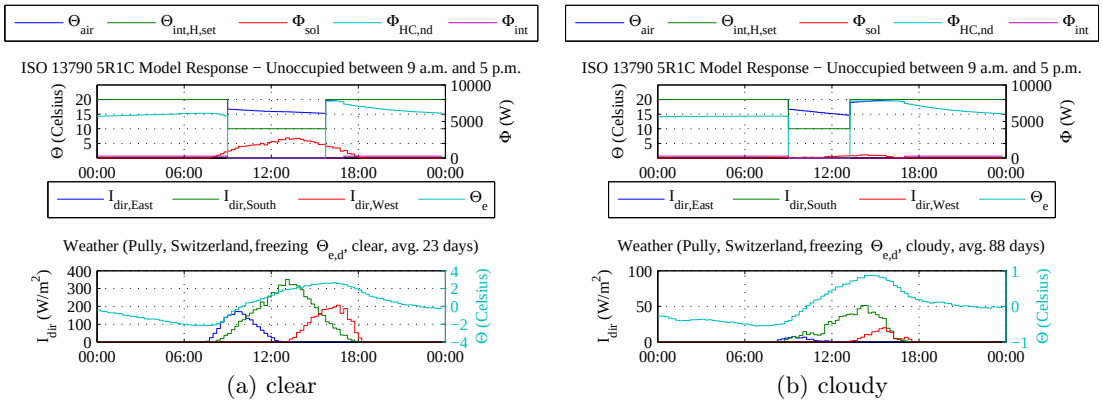

Fig. 17. ISO 13790 response: Freezing temperature, H-U$_{low}$.

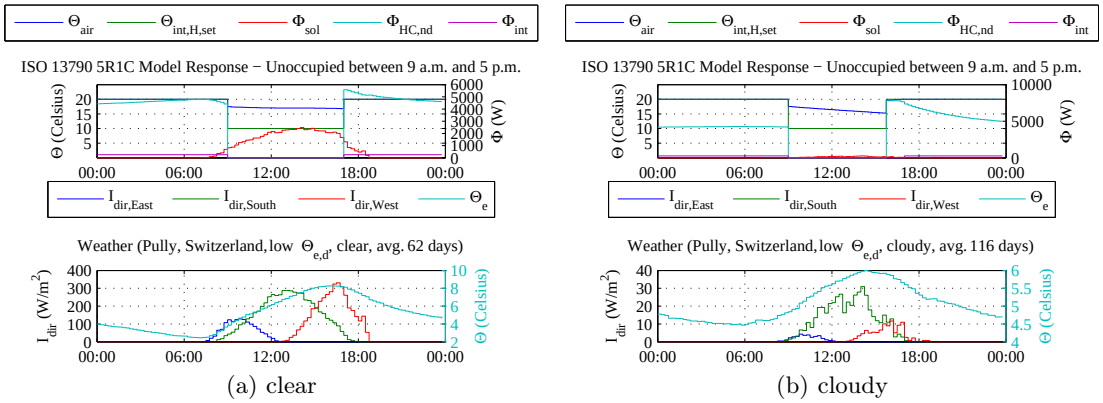

Fig. 18. ISO 13790 response: Low temperature, H-U$_{low}$.

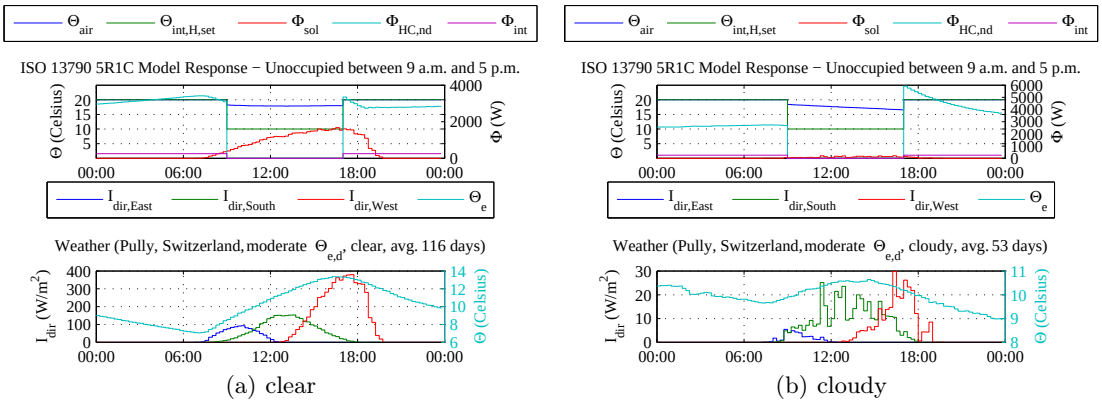

(a) clear (b) cloudy

Fig. 19. ISO 13790 response: Moderate temperature, H-U$_{low}$.

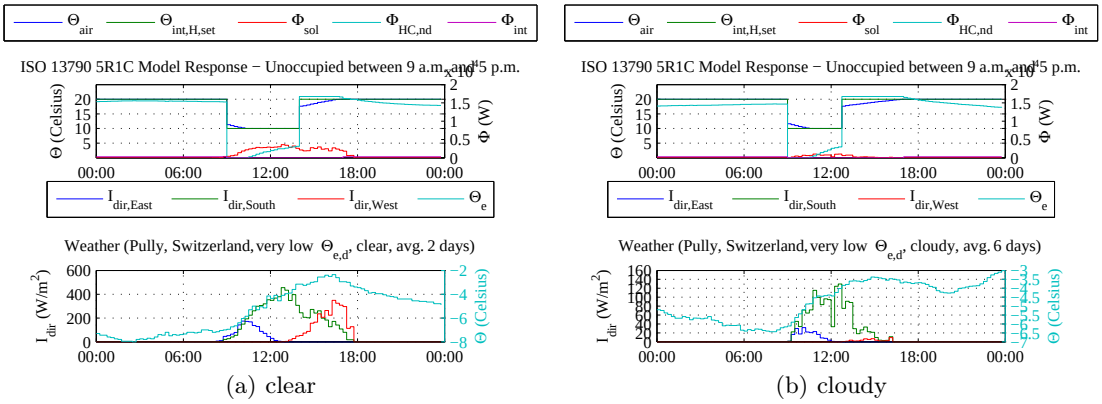

(a) clear (b) cloudy

Fig. 20. ISO 13790 response: Very low temperature, H-U$_{high}$.

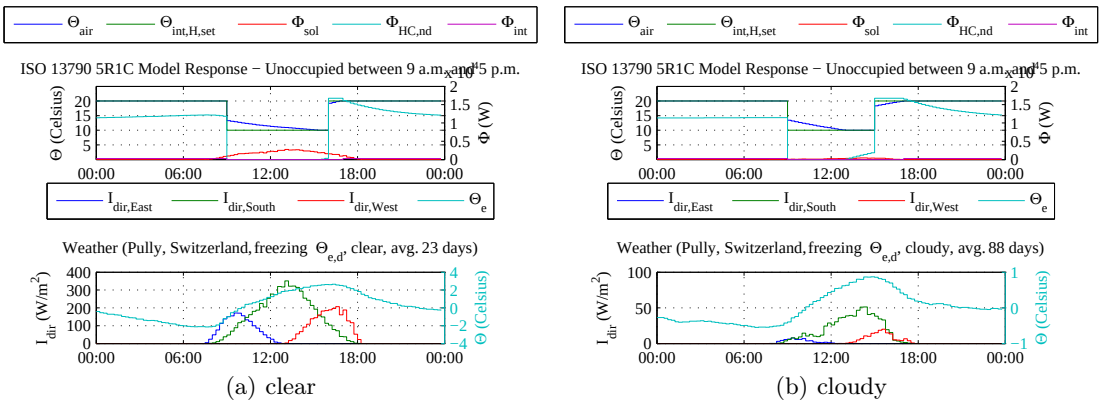

(a) clear (b) cloudy

Fig. 21. ISO 13790 response: Freezing temperature, H-U$_{high}$.

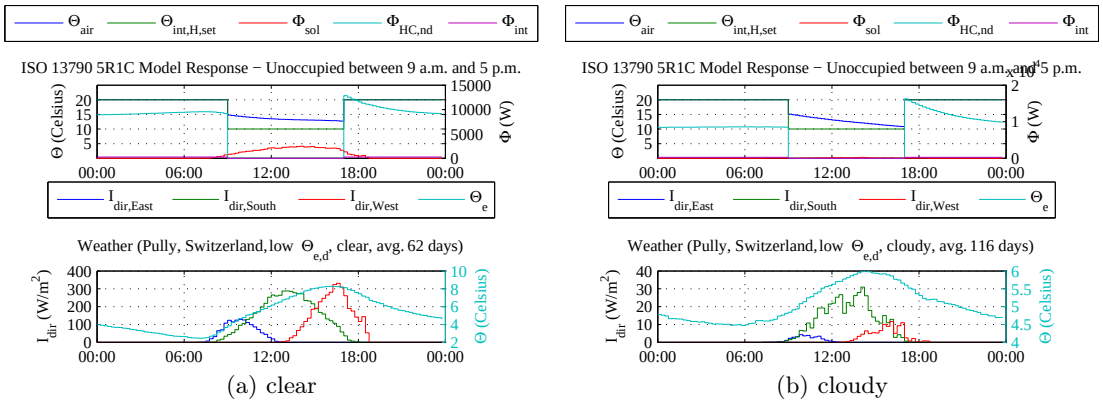

(a) clear (b) cloudy

Fig. 22. ISO 13790 response: Low temperature, H-U$_{high}$.

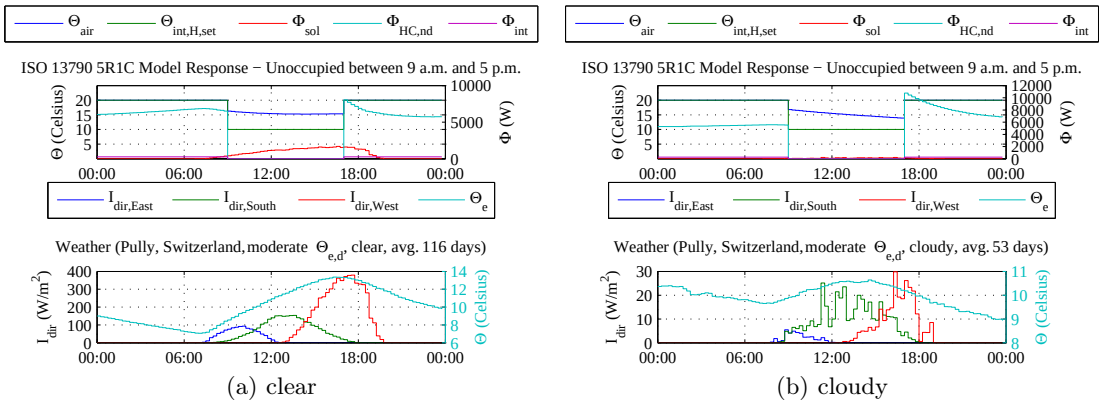

(a) clear (b) cloudy

Fig. 23. ISO 13790 response: Moderate temperature, H-U$_{high}$.